Biochemistry

pubs.acs.org/biochemistry
Article

Crystal Structure and Enzymology of *Solanum tuberosum* Inositol Tris/Tetrakisphosphate Kinase 1 (*St*ITPK1)

Hayley L. Whitfield, Raquel Faba Rodriguez, Megan L. Shipton, Arthur W.H. Li, Andrew M. Riley, Barry V.L. Potter, Andrew M. Hemmings,* and Charles A. Brearley*

Cite This: *Biochemistry* 2024, 63, 42−52

ABSTRACT: Inositol phosphates and their pyrophosphorylated derivatives are responsive to the phosphate supply and are agents of phosphate homeostasis and other aspects of physiology. It seems likely that the enzymes that interconvert these signals work against the prevailing milieu of mixed populations of competing substrates and products. The synthesis of inositol pyrophosphates is mediated in plants by two classes of ATP-grasp fold kinase: PPIP5 kinases, known as VIH, and members of the inositol tris/tetrakisphosphate kinase (ITPK) family, specifically ITPK1/2. A molecular explanation of the contribution of ITPK1/2 to inositol pyrophosphate synthesis and turnover in plants is incomplete: the absence of nucleotide in published crystal structures limits the explanation of phosphotransfer reactions, and little is known of the affinity of potential substrates and competitors for ITPK1. Herein, we describe a complex of ADP and *St*ITPK1 at 2.26 Å resolution and use a simple fluorescence polarization approach to compare the affinity of binding of diverse inositol phosphates, inositol pyrophosphates, and analogues. By simple HPLC, we reveal the novel catalytic capability of ITPK1 for different inositol pyrophosphates and show Ins(3,4,5,6)P_4 to be a potent inhibitor of the inositol pyrophosphate-synthesizing activity of ITPK1. We further describe the exquisite specificity of ITPK1 for the *myo*-isomer among naturally occurring inositol hexakisphosphates.

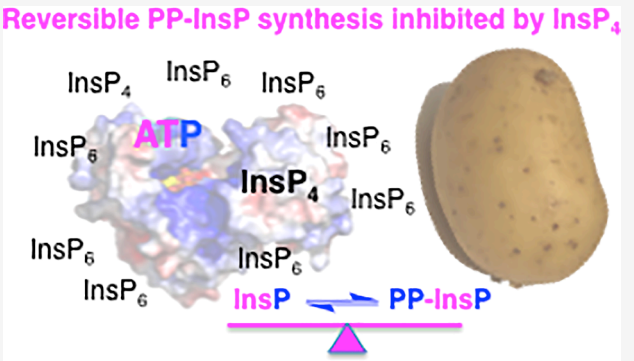

INTRODUCTION

Since the discovery of inositol pyrophosphates (diphosphoinositol phosphates) in plants,[1,2] inositol pyrophosphates have emerged as participants in diverse aspects of plant physiology extending to phosphate starvation response, hormone signaling, symbiosis, and response to pathogens.[3−10] The same can also be claimed of inositol phosphates lacking anhydride bonds.[3,11−15] The claim of the contribution of inositol pyrophosphates to aspects of plant biology rests heavily on the characterization of enzymes and the analysis of mutants thereof. ITPKs and PPIP5Ks, variously referred to as VIH or Vip1 in plants and yeast, respectively, contribute to inositol pyrophosphate synthesis. Both possess the ATP-grasp fold. PPIP5Ks contain an additional histidine acid phosphatase domain.[16]

The catalytic potential of plant ITPKs is particularly diverse[17−22] when compared with the kinase activity of VIH1/2, considered only to act on $InsP_6$ and 5-$InsP_7$, 5-PP-Ins(1,2,3,4,6)P_5, hereafter 5-PP-$InsP_5$. For plants, VIH1/2 analysis has been restricted to isolated domains.[23,24] Like other inositol phosphate kinases, IP6K[25] and IP5K (IPK1),[26] ITPKs are reversible phosphotransferases[21,22,27] as is the ATP-grasp kinase domain of PPIP5K.[28] Consideration of reversibility under prevailing physiological conditions, with usually poorly defined nucleotide status, has the consequence that the causative signaling species among ITPK and VIH substrates and products are difficult to decipher.

In vitro, *At*ITPK1 shows greater ATP-synthesis from 5-PP-$InsP_5$ than 5-PP-$InsP_5$ synthesis from $InsP_6$.[27] These activities are, however, a very small fraction of the Ins(3,4,5,6)P_4 1-kinase activity of the enzyme.[21] To date, the only enzymes capable of synthesizing $InsP_8$, 1,5-$InsP_8$, 1,5-$[PP]_2$-Ins-(2,3,4,6)P_4, hereafter 1,5-$[PP]_2$-$InsP_4$, the presumed endogenous $[PP]_2$-$InsP_4$ in plants,[3] are the VIH1/2 enzymes.[23,24] Even so, the activities of ITPK1/2 and VIH1/2[20,21,27] do not account for the full spectrum of inositol pyrophosphates detected in plants.[21,27,34] The possible isomers and enantiomers comprise 1-$InsP_7$, 1-PP-Ins(2,3,4,5,6)P_5, hereafter 1-PP-$InsP_5$; 3-$InsP_7$, 3-PP-Ins(1,2,4,5,6)P_5, hereafter 3-PP-$InsP_5$; 4-$InsP_7$, 4-PP-Ins(1,2,3,5,6)P_5, hereafter 4-PP-$InsP_5$; and 6-$InsP_7$, 6-PP-Ins(1,2,3,4,5)P_5, hereafter 6-PP-$InsP_5$. The *meso*-

Received: July 30, 2023
Revised: November 30, 2023
Accepted: November 30, 2023
Published: December 26, 2023

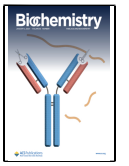

https://doi.org/10.1021/acs.biochem.3c00404
Biochemistry 2024, 63, 42−52

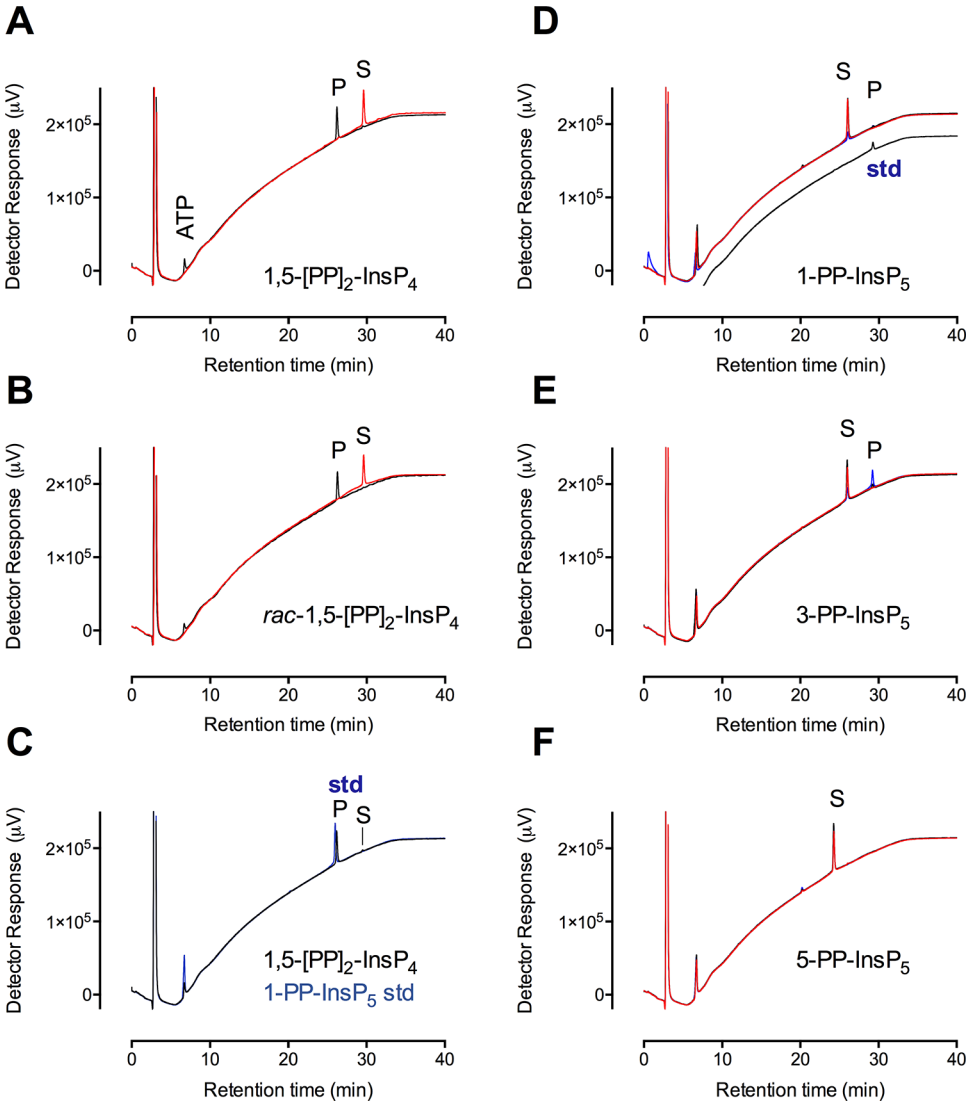

Figure 1. *St*ITPK1 is a reversible inositol pyrophosphate-ADP phosphotransferase. HPLC resolution of products of 12h reaction of *St*ITPK with ADP and (A) 1,5-$[PP]_2$-$InsP_4$; (B) *rac*-1,5-$[PP]_2$-$InsP_4$. Products of the dephosphorylation of 1,5-$[PP]_2$-$InsP_4$ coelute with 1-PP-$InsP_5$, (C). Substrates are indicated, S and products, P. Chromatograms of reactions without enzyme are shown in red, with enzyme in black and chromatograms of standards are shown in blue. The position of elution of ATP formed by phosphotransfer to ADP is shown in panel A. ADP elutes in the solvent front. The standards showing the elution position of PP-$InsP_5$ in C contain ATP. The ATP peaks in all other panels are products of phosphotransfer from substrate to ADP. HPLC of products of reaction of *St*ITPK1 with ATP and 1-PP-$InsP_5$, 3-PP-$InsP_5$, or 5-PP-$InsP_5$ are shown in D, E and F. Here, chromatograms of 3 h incubations with enzyme are shown in black, and 12 h incubations are shown in blue. The position of a 1,5-$[PP]_2$-$InsP_4$ standard (trace offset on the *y*-axis) is shown in panel D. The HPLC column was eluted with a gradient of HCl.

isomers include 5-PP-$InsP_5$ and 2-$InsP_7$, 2-PP-Ins(1,3,4,5,6)P_5, and hereafter 2-PP-$InsP_5$.

The ITPK family, including members that synthesize inositol pyrophosphates[20,21,27] or do not,[20,22] is represented in early land plants[29] and in early aquatic vascular plants, the duckweeds in which a lipid-independent pathway of $InsP_6$ synthesis that uses the favored $InsP_4$ substrate of plant ITPK1[21] was described.[30−32] Herein, we have solved a crystal structure for a potato enzyme, *St*ITPK1, in complex with ADP. We show the enzyme's preference for $InsP_4$ over $InsP_6$ and PP-InsP substrates and describe a simple, yet powerful, fluorescence polarization approach that could advance the study of other ATP-grasp kinases.

MATERIALS AND METHODS

Details of protein purification, enzyme assays, HPLC analysis of reaction products, ligand-binding assays, and X-ray crystallography can be found in the Supporting Information.

RESULTS

***St*ITPK1 Displays Phosphokinase Activity.** The structures of compounds tested as substrates, ligands, or inhibitors of *St*ITPK1 and *At*ITPK1 are shown in Figure S1). *St*ITPK1 is similar to *At*ITPK1: generating 5-PP-$InsP_5$ from $InsP_6$ (Figure S2A), lacking activity against Ins(1,2,3,5,6)P_5 (Figure S2B) and showing phosphokinase activity against the enantiomer Ins(1,2,3,4,5)P_5, yielding a product that eluted before $InsP_6$ (Figure S2C).

Multiple inositol hexakisphosphate isomers are present in soil. In addition to *myo*-$InsP_6$, D-*chiro*-$InsP_6$, *neo*-$InsP_6$, and

https://doi.org/10.1021/acs.biochem.3c00404
Biochemistry 2024, 63, 42−52

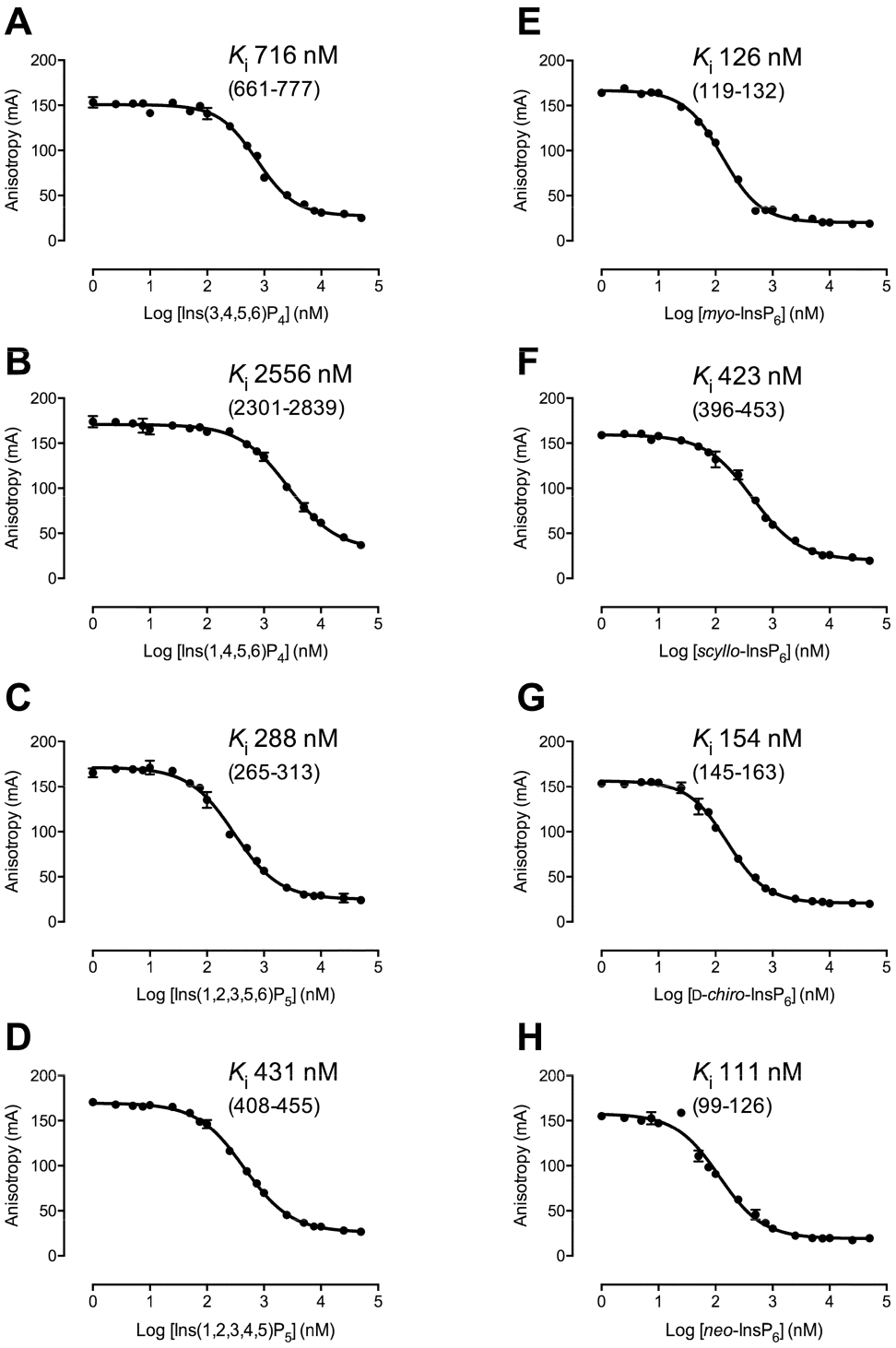

Figure 2. High-affinity binding of inositol phosphates to *St*ITPK1. Displacement of 2-FAM-InsP_5 with (A) Ins(3,4,5,6)P_4; (B) Ins(1,4,5,6)P_4; (C) Ins(1,2,3,5,6)P_5; (D) Ins(1,2,3,4,5)P_5; (E) *myo*-InsP_6; (F) *scyllo*-InsP_6; (G) D-*chiro*-InsP_6; and (H) *neo*-InsP_6. Data are the means and standard deviations of four replicate measurements; K_i (nM) with confidence interval (nM) in parentheses.

scyllo-InsP_6 have been identified.[33] Their presence is unexplained, but because plant matter is a major input to the soil we tested whether they might be substrates for *St*ITPK1. Among isomers of inositol hexakisphosphate, *St*ITPK1 phosphorylates the *myo*-isomer only (Figure S2A,D−F). The lack of activity toward other inositol hexakisphosphates described in the soil makes it unlikely that this ancestral plant enzyme, present in liverworts, bryophytes, and early vascular aquatic plants,[29] could contribute to the presence of noncanonical inositol pyrophosphates in soil, should they be found.

***St*ITPK1 Displays Stereospecific [PP]$_2$-InsP_4/ADP Phosphotransferase Activity.** Recently, noncanonical PP-InsP_5 species have been identified in plants.[27,34] CE-MS peaks with chromatographic mobility and parent/daughter ion relationships identical with synthetic D- and/or L-4-PP-InsP_5 [4-PP-InsP_5/6-PP-InsP_5] and the *meso*-compound 2-PP-InsP_5 have been detected.[27,34] Similar conclusions can be drawn from

https://doi.org/10.1021/acs.biochem.3c00404
Biochemistry 2024, 63, 42−52

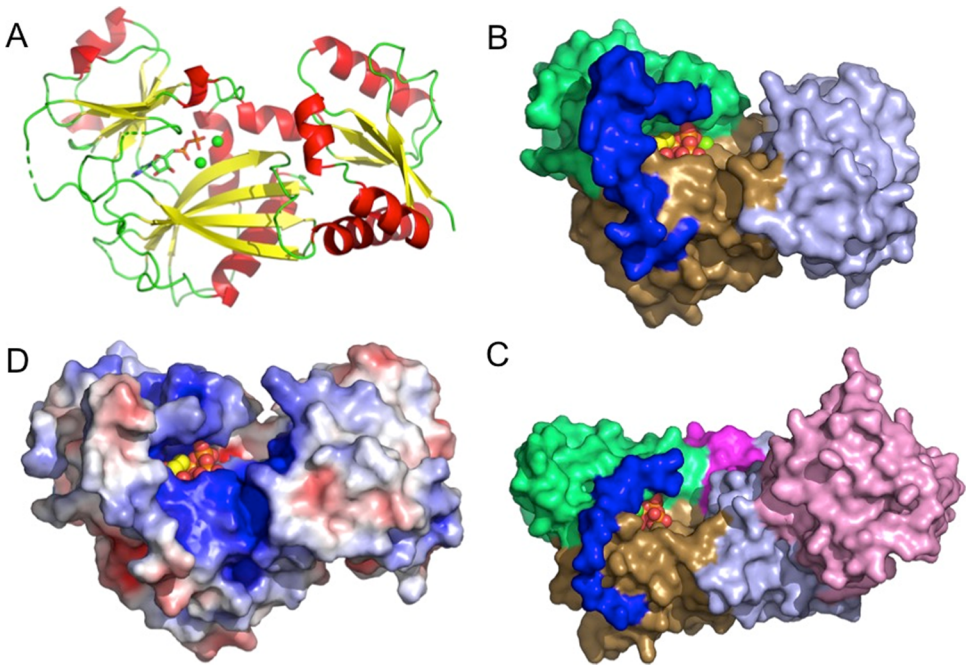

Figure 3. Overview of the crystal structure of *St*ITPK1. (A) Cartoon representation of the structure of *St*ITPK1, colored by secondary structure (α-helix red, β-sheet yellow, and coil green). Broken lines in the backbone trace indicate residues that were unresolved in the model due to disorder. Bound nucleotide is shown in stick format with coloring as follows: carbon-green, oxygen-red, nitrogen-blue, and phosphorus-orange. (B) Molecular surface representation of the structure of *St*ITPK1 colored by subdomain. Subdomains are the kinase N-terminal domain (light blue), kinase central domain (lime green) and kinase central domain (sand). Here and in panel D, the polypeptide connecting the central and C-terminal domains is colored dark blue. Bound ADP is shown in atom sphere format. (C) Molecular surface representation of the structure of *At*ITPK4 (PDB: 7PUP). Coloring as in panel C except that the additional HAD domain found in this enzyme is colored pink and the tab insertion unique to ITPK4s is colored magenta. (D) Molecular surface of *St*ITPK1 colored by electrostatic potential (red-acidic, blue-basic). The orientation of the molecule is the same as that in panel A. In panels B−D, bound ADP is shown in atom sphere format and colored according to that in panel A.

a previous study.[21] It is, however, unknown whether plants possess a single $[PP]_2$-$InsP_4$, a mixture of the enantiomers 1,5-$[PP]_2$-$InsP_4$/3,5-$[PP]_2$-$InsP_4$ or additional isomers and enantiomeric pairs.[3] Recent work has identified a family of 5-β-phosphate-targeting phosphatases,[34] showing that VIH1/2 is not the only agent of $[PP]_2$-$InsP_4$ turnover. Moreover, it is also unclear whether plant $[PP]_2$-$InsP_4$s are substrates for phosphotransfer to ADP. The known reversibility of phosphokinase activity of *At*ITPK1[21,27] prompted us to test the same of *St*ITPK1. We did so because the presence of 1-PP-$InsP_5$ and/or 3-PP-$InsP_5$ in plants[21,27] could also arise from dephosphorylation of 1,5-$[PP]_2$-$InsP_4$ ($InsP_8$) and/or 3,5-$InsP_8$, 3,5-$[PP]_2$-Ins(1,2,4,6)P_4, hereafter 3,5-$[PP]_2$-$InsP_4$. We tested the ability of *St*ITPK1 to effect phosphotransfer from 1,5-$[PP]_2$-$InsP_4$ and a racemic mixture of the two enantiomers, hereafter termed *rac*-1,5-$[PP]_2$-$InsP_4$ (Figure 1). *St*ITPK1 showed phosphotransfer (to ADP) activity against 1,5-$[PP]_2$-P_4, yielding 1-PP-$InsP_5$ and ATP (Figure 1A,C). The same was true for *rac*-1,5-$[PP]_2$-$InsP_4$ (Figure 1B,C). Full conversion of *rac*-1,5-$[PP]_2$-$InsP_4$ (ie., of both 1,5-$[PP]_2$-$InsP_4$ and its enantiomer 3,5-$[PP]_2$-$InsP_4$) shows that both enantiomers are substrates, with enzyme attack on the 5-β-position of both. Consistent with this attack on the 5-β-phosphate, neither of the nonhydrolyzable 1,5-$[PA]_2$-Ins(2,3,4,6)P_4, hereafter [1,5-$[PA]_2$-$InsP_4$, nor 1,5-$[PCP]_2$-Ins(2,3,4,6)P_4, hereafter 1,5-$[PCP]_2$-$InsP_4$, analogues were substrates (Figure S3E,F). Both compounds eluted substantially earlier than 3-PP-$InsP_5$ (or its enantiomer, 1-PP-$InsP_5$) (Figure S3). Similar observations were made for *At*ITPK1 (Figure S3). Here, both chiral- and racemic 1,5-$[PP]_2$-$InsP_4$ were substrates for phospho-transfers from the *meso*-5-position, yielding 1-PP-$InsP_5$/3-PP-$InsP_5$ and ATP products. Again, the nonhydrolyzable $[PA]_2$- and $[PCP]_2$-analogues were not substrates (Figure S3C,D). These results extend the repertoire of phosphotransfer reactions catalyzed by *At*ITPK1, two groups have shown transfer of the γ-phosphate of ATP to the 5-phosphate of $InsP_6$ and vice versa, from the β-position of 5-PP-$InsP_5$ to the β-phosphate of ADP.[21,27] The two studies arrived at very similar values of K_{cat} (rate constant) for phosphorylation of $InsP_6$ and the latter derived K_{cat} for ATP-synthesis that is double that for 5-PP-$InsP_5$ production.

***St*ITPK1 and *At*ITPK1 Display Stereospecific Phosphokinase Activity against PP-InsPs.** Surprisingly, given the current dogma that $[PP]_2$-$InsP_4$ synthesis belongs only to VIH1/2, we found 1-PP-$InsP_5$ and 3-PP-$InsP_5$ both to be phosphokinase substrates of *St*ITPK1 incubated with ATP (Figure 1D,E) with 1-PP-$InsP_5$ the weaker substrate. Both yielded products, 1,5-$[PP]_2$-$InsP_4$ and 3,5-$[PP]_2$-$InsP_4$, respectively, that coeluted with a 1,5-$[PP]_2$-$InsP_4$ standard (Figure 1D). To confirm the commonality of this activity, we also tested *At*ITPK1 for the same activity. Like *St*ITPK1, *At*ITPK1 also showed stronger activity against 3-PP-$InsP_5$, generating a product with the chromatographic properties of 3,5-$[PP]_2$-$InsP_4$ (Figure S4). Neither *St*ITPK1 (Figure 1F) nor *At*ITPK1 (Figure S4C) phosphorylated 5-PP-$InsP_5$. These observations establish an exchange of phosphate between the γ-position of ATP and a "vacant β-position" on PP-$InsP_5$ species present in plants and vice versa, viz. transfer of a β-phosphate from $[PP]_2$-$InsP_4$ to the "vacant γ-position" of ADP. That the activity resides with ITPK1 is wholly consistent with the role of ITPK1

https://doi.org/10.1021/acs.biochem.3c00404
Biochemistry 2024, 63, 42−52

as a master regulator of phosphate starvation response.[15,27] The physiological balance of such reactions will be dependent on the concentrations of nucleotides and inositol pyrophosphates.

Ligand-Binding Assay Allows Comparison of Binding of Diverse Inositol Phosphates and Inositol Pyrophosphates to ATP-Grasp Kinases. To determine the relative strengths of binding of different inositol phosphate and inositol pyrophosphate substrates of *St*ITPK1, we undertook fluorescence polarization experiments with 2-FAM-InsP_5.[35] This molecule has proved a useful probe of the active and/or inositol phosphate-binding sites of enzymes as diverse as SHIP2[36] and IP5K (*At*IPK1),[37] and HDAC complexes.[35] A saturation curve for the binding of 2-FAM-InsP_5 to *St*ITPK1 is shown in Figure S5, and displacement curves are shown for diverse inositol phosphates in Figure 2. The structures of these compounds are shown in Figure S1.

K_i ranged from 111 nM for *neo*-InsP_6 (Figure 2H) to 2556 nM for Ins(1,4,5,6)P_4 (Figure 2B). K_i values increased, broadly, InsP_6 < InsP_5 < InsP_4. Consistent with enzymatic data for *At*ITPK1,[21] Ins(3,4,5,6)P_4, the better substrate of the two enantiomers, bound much more tightly with K_i of 716 nM (Figure 2A) than Ins(1,4,5,6)P_4 (Figure 2B). Interestingly, the two InsP_5s also displayed similar binding affinity (K_i values of 288 nM for Ins(1,2,3,5,6)P_5 and 431 nM for Ins(1,2,3,4,5)P_5) (Figure 2C,D) against enzyme activity for the latter only (Figure S2). Among inositol hexakisphosphates, with the exception of the *scyllo*-stereoisomer (Figure 2F), all bound with similar affinity with K_i in the range 111−154 nM (Figure 2E−H); *scyllo*-InsP_6 (423 nM).

We rationalize the failure of *St*ITPK1 to phosphorylate *neo*-InsP_6 (Figure S2D), with its two axial phosphates in the plane of symmetry, equivalent to the axial 2-phosphate and equatorial 5-phosphate of *myo*-InsP_6 (Figure S1), as being consistent with the requirement for an equatorial 5-phosphate in the single *myo*-InsP_5 substrate, Ins(1,2,3,4,5)P_5. The failure of *St*ITPK1 to phosphorylate *scyllo*-InsP_6 (Figure S2F), a C2-epimer of *myo*-InsP_6 with six equatorial phosphates (Figure S1), suggests a requirement for phosphokinase substrates to possess a single axial phosphate in the plane of symmetry (for *myo*-InsP_6, in the 2-position). Consistent with this, D-*chiro*-InsP_6, which has two axial phosphates in *trans*, was also not a substrate (Figure S2E).

Consistent with the displacement data and previous study of *At*ITPK1,[21] Ins(3,4,5,6)P_4 proved a better substrate than both its enantiomer Ins(1,4,5,6)P_4 and InsP_6 (Figure S6). Discrimination between the InsP_4 enantiomers was ∼200-fold in favor of Ins(3,4,5,6)P_4 for both *St*ITPK1 and *At*ITPK1 (Figure S6). This enantioselectivity is reversed for *At*ITPK4.[22] For both *St*ITPK1 and *At*ITPK1, InsP_6 proved to be a better phosphokinase substrate than Ins(1,4,5,6)P_4 is a hydroxykinase substrate (Figure S6).

Nucleotide-Liganded Structure of *St*ITPK1 Allows Modeling of Phosphotransfer Reactions of Plant ITPK1. Crystal structures have been reported for two plant ITPKs, *At*ITPK4 (PDB: 7PUP) and *Zm*ITPK1 (PDB: 7TN8).[22,38] The former lacks bound inositol phosphate, and the latter lacks bound nucleotide. To explain the interaction of ITPK1 with nucleotide cosubstrate, the *St*ITPK1 crystal structure (residues 8−320) was solved in space group C222 with a monomer of the enzyme in the asymmetric unit (Figure 3) (PDB 8OXE). Refined against all data to 2.26 Å resolution, the final structural model had an *R*-factor of 19.0% (Rfree 24.1%) (Table S1). As expected, *St*ITPK1 adopts the ATP-grasp kinase fold with three conserved subdomains referred to here as N-terminal, central, and C-terminal domains, following the nomenclature previously applied in descriptions of the crystal structures of ITPK1 orthologs.[22,38−40]

Relative to *At*ITPK4, ITPK1 possesses a "tether" insertion following the central subdomain, while AtITPK4 possesses a "tab" in the N-terminal subdomain.[22] The tether comprises a polypeptide connection between the C-terminal β-strand of the central domain and a helix of the C-terminal domain running under the protein. This polypeptide lies across the top of the active site cavity, linking the two domains (Figure 3B,D). In all the ITPK1s of known molecular structure where this polypeptide is resolved, it provides residues that contribute to the ATP cofactor/substrate binding pocket. Consistent with the absence of the resolved nucleotide, this region is disordered in the crystal structure of *Zm*ITPK1,[38] but in *St*ITPK1, it is stabilized in most parts by adventitious interactions with a neighboring copy of the molecule in the crystal lattice. Both the tab and tether insertions help shape the active site cleft in plant ITPK1 and ITPK4, suggesting that they may contribute to differential substrate recognition (Figure 3B,C). As for other ITPK1 enzymes, the active site of *St*ITPK1 is narrow, unlike the more open active site in *At*ITPK4 (Figure S7), and features a highly positively charged active site (Figure 3D).

To explain the preference of *St*ITPK1 for its substrates we modeled the binding of the Ins(1,4,5,6)P_4 and Ins(3,4,5,6)P_4 enantiomers to *St*ITPK1, adopting the consensus specificity subsite nomenclature.[39] Briefly, subsite A is the site of phosphoryl transfer and constitutes the catalytic center. For Ins(1,4,5,6)P_4 (Figure 4A), substituents on locants 3, 2, 1, 6, 5, and 4 of the *myo*-inositol ring occupy sites A, B, C, D, E, and F, respectively, while for Ins(3,4,5,6)P_4 (Figure 4B), substituents on locants 1, 6, 5, 4, 3, and 2 occupy sites A, B, C, D, E, and F, respectively. Residues forming polar interactions with the hydroxyl and phosphate groups of the substrates in the relaxed models are summarized (Table S2). The predicted pose of the poor substrate, Ins(1,4,5,6)P_4, lacks polar interactions in the B- and C-subsites (Figure 4A), while the strong substrate, Ins(3,4,5,6)P_4, enjoys polar interactions in all subsites except F, occupied by the 2-hydroxyl group (Figure 4B). In the B-pocket, the 6-phosphate of Ins(3,4,5,6)P_4 is predicted to interact with the side chain of Asn272. The substitution of a conserved glycine residue at this site in the ITPK4s (Gly437 in *At*ITPK4) may help explain the poor activity of *At*ITPK4 toward this potential substrate. If accurately predicted, these interactions in the B- and C-subsites are likely crucial for enantiospecific hydroxy-kinase activity by *St*ITPK1 toward inositol tetrakisphosphates.

A model for a stereochemically productive complex of InsP_6 with *St*ITPK1 derived by molecular docking is shown in Figure S8. All residues observed to interact with InsP_6 in its complex with the maize enzyme[38] are conserved in *St*ITPK1. However, due to the lack of bound nucleotide in the crystal structure of *Zm*ITPK1, the central domain is displaced relative to that seen in the potato enzyme structure and InsP_6 binds in such a way that in-line phosphoryl transfer from the γ-phosphate of ATP is implausible.[39,41] It, therefore, appears that the absence of a nucleotide from the structure of the complex of *Zm*ITPK1 with InsP_6 leads to a situation where an unproductive binding mode is stabilized. On the other hand, in the pose of InsP_6 predicted for *St*ITPK1, InsP_6 binds with its "receiving" 5-phosphate in

https://doi.org/10.1021/acs.biochem.3c00404
Biochemistry 2024, 63, 42−52

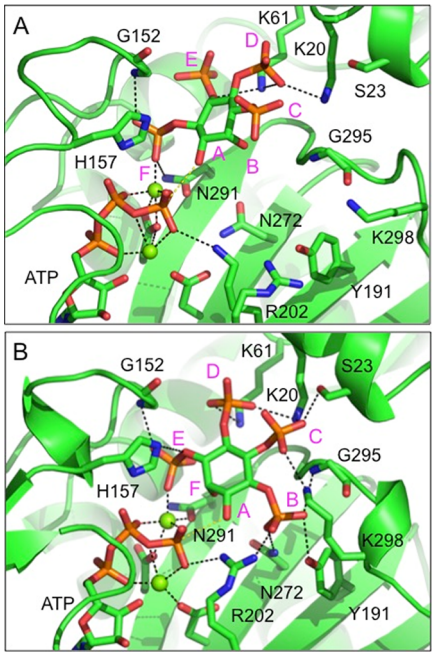

Figure 4. Prediction of the binding modes of an enantiomeric pair of substrates in the active site of *St*ITPK1. (A) Closeup view of the energy minimized predicted binding mode of the poor substrate, Ins(1,4,5,6)P_4, in the kinase domain active site. The enzyme is shown in the cartoon format and colored green. The substrate and active site residues (labeled) with which it forms polar interactions are shown in the stick format with carbon colored green, oxygen red, nitrogen blue, and phosphorus orange. Magnesium ions are shown as dark green spheres. Polar interactions are indicated by black dashed lines. Specificity subsites are labeled A−F (magenta font) such that the hydroxyl group positioned to accept the γ-phosphate of ATP by in-line transfer (the hydroxyl attached to carbon 3 of the inositol ring, in this case) occupies subsite A and the remaining subsites are arrayed in an anticlockwise sense when observed from the viewpoint adopted in this figure. (B) View of the energy minimized predicted binding mode of the good substrate, Ins(3,4,5,6)P_4, in the kinase domain active site. The hydroxyl attached to carbon 1 of the inositol ring, in this case, occupies subsite A. Display format and coloring as in panel A.

the F-specificity subsite (Figure S8), contrasting with the "receiving" 1-hydroxyl of Ins(3,4,5,6)P_4 which occupies subsite A (Figure 4). The minimum distance in this pose from the γ-phosphate phosphorus atom of ATP to the 5-phosphate oxygen of the substrate is a little over 3.5 Å, rendering plausible in-line phosphoryl transfer from the γ-phosphate of ATP to generate the observed 5-PPInsP$_5$ product. Again, polar contacts to the ligand are made by Q224 of the tether region; thus, the bound nucleotide may stabilize the central subdomain and a portion of the tether, enabling recognition of InsP$_6$ and catalysis. In *Zm*ITPK1, the tether is part of a catalytic specificity element that sanctions phosphokinase activity against InsP$_6$.[38] The absence of the tether polypeptide in ITPK4 would then be consistent with its inability to synthesize inositol pyrophosphates.[20,22]

PP-InsP Analogues Confirm the Stereospecificity of *St*ITPK1 for Phosphorylation of PP-InsPs. For both *St*ITPK1 and *At*ITPK1, InsP$_6$ was the strongest phosphokinase substrate, with 3-PP-InsP$_5$ being a stronger substrate than 1-PP-InsP$_5$, whereas 5-PP-InsP$_5$ was not a substrate (Figures 1 and S4, Table S3). Nevertheless, the three PP-InsP$_5$s tested showed similar K_i values for displacement of 2-FAM-InsP$_5$ from *St*ITPK1, in the range 88−178 nM (Figure S9A−C). Overall, PP-InsP$_5$s displayed similar K_i values to InsP$_6$ isomers (cf. Figures 2 and S9). We also tested a range of PP-InsP analogues as phosphokinase substrates (Figure 5). Interestingly, both 3-PCP-Ins(1,2,4,5,6)P_5, hereafter 3-PCP-InsP$_5$, and 1-PCP-Ins(2,3,4,5,6)P_5, hereafter 1-PCP-InsP$_5$, were substrates. They yielded products, with identical retention times, that we assume to be 3-PCP-, 5-PP-Ins(1,2,4,6)P_4 and 1-PCP-, 5-PP-Ins(2,3,4,6)P_4 respectively (Figure 5A,B). *At*ITPK1 also displays the same preference for enantiomers of PCP-InsP$_5$ analogues (Figure S4).

For both *St*ITPK1 and *At*ITPK1, 3-PCP-InsP$_5$, and 1-PCP-InsP$_5$ were better substrates than their "parents" 3-PP-InsP$_5$ and 1-PP-InsP$_5$ (cf. Figures 5 and S4), although both compounds gave K_i for displacement of 2-FAM-InsP$_5$ between 2 and 4-times higher than the "parents" (Figure S9). For *St*ITPK1, 5-PA-Ins(1,2,3,4,6)P_5, hereafter 5-PA-InsP$_5$, was the strongest phosphokinase substrate after *myo*-InsP$_6$ (Figure 5C, Table S3), but was a weak substrate for *At*ITPK1 (Figure S4G). From this compound, both enzymes generated a single product that eluted shortly after *myo*-InsP$_6$ and substantially before 5-PP-InsP$_5$. Retention between InsP$_6$ and 5-PP-InsP$_5$ is indicative of pyrophosphorylation, with the nonreactive phosphono-acetoxy group (on the 5-position) likely contributing a little less to interaction with the column than a 5-phosphomonoester.

Of the other PP-InsP$_5$ analogues, 5-PCH$_2$Am-Ins(1,2,3,4,6)-P_5, hereafter 5-PCH$_2$Am-InsP$_5$, and 1-PA-Ins(2,3,4,5,6)P_5, hereafter 1-PA-InsP$_5$, were very weak substrates (Figure 5D,F), while 5-PCF$_2$Am-Ins(1,2,3,4,6)P_5, hereafter 5-PCF$_2$Am-InsP$_5$, was not a substrate (Figure 5E). 5-PCH$_2$Am-InsP$_5$ and 5-PCF$_2$Am-InsP$_5$ displaced 2-FAM-InsP$_5$ from *St*ITPK1 with K_i of 889 and 106 nM, respectively (Figure S9E,F), while 1-PA-InsP$_5$ displaced 2-FAM-InsP$_5$ with a K_i of 300 nM. For 5-PCP-Ins(1,2,3,4,6)P_5, hereafter 5-PCP-InsP$_5$, a K_i of 101 nM was obtained (Figure S9D), and for 5-PP-InsP$_5$, a K_i of 162 nM was obtained (Figure S9C). These observations are consistent with polar contacts for the bridging anhydride oxygen atom of 5-PP-InsP$_5$ and the fluorine atom(s) of 5-PCF$_2$Am-InsP$_5$, with these being absent for the hydride H atom(s) of 5-PCH$_2$Am-InsP$_5$. The electron-withdrawing effect of the fluorine atoms might also be expected to increase the negative charge density of the terminal phosphonate in 5-PCF$_2$Am-InsP$_5$. Irrespective of whether molecules were substrates or not, inositol phosphates, inositol pyrophosphates, and analogues, alike, were inhibitors of the Ins(1,2,3,4,5)P_5 and InsP$_6$ phosphokinase activity of *St*ITPK1 with inhibition for this assay falling in the range 42−89% (Figure 6, Table S3).

Example HPLC traces showing reduced generation of presumed 5-PP-InsP$_4$ product from Ins(1,2,3,4,5)P_5[21] on the inclusion of 1-PCP-InsP$_5$ or 3-PCP-InsP$_5$ are presented (Figure S10). Both 1-PCP-InsP$_5$ and 3-PCP-InsP$_5$ are potent inhibitors (Figures 6 and S10, Table S3), confirming the predictive power of the fluorescence polarization assays which yielded a lower K_i for 3-PCP-InsP$_5$ than for 1-PCP-InsP$_5$, both lower than that for Ins(1,2,3,4,5)P_5 (cf. Figures 2D and S9G,H). Consistent with this, the 3-PCP-analogue was also the more potent inhibitor of Ins(1,2,3,4,5)P_5 phosphokinase activity (Figures 6A and S10B,C, Table S3). In the absence of an inhibitor, turnover of Ins(1,2,3,4,5)P_5 and InsP$_6$ were similar giving K_{cat} of 0.94 ± 0.03 and 1.14 ± 0.07 min^{-1}. Of all the compounds tested against InsP$_6$ (Figure 6B and Table S3), Ins(3,4,5,6)P_4, K_i 716 nM, was a particularly powerful inhibitor

https://doi.org/10.1021/acs.biochem.3c00404
Biochemistry 2024, 63, 42−52

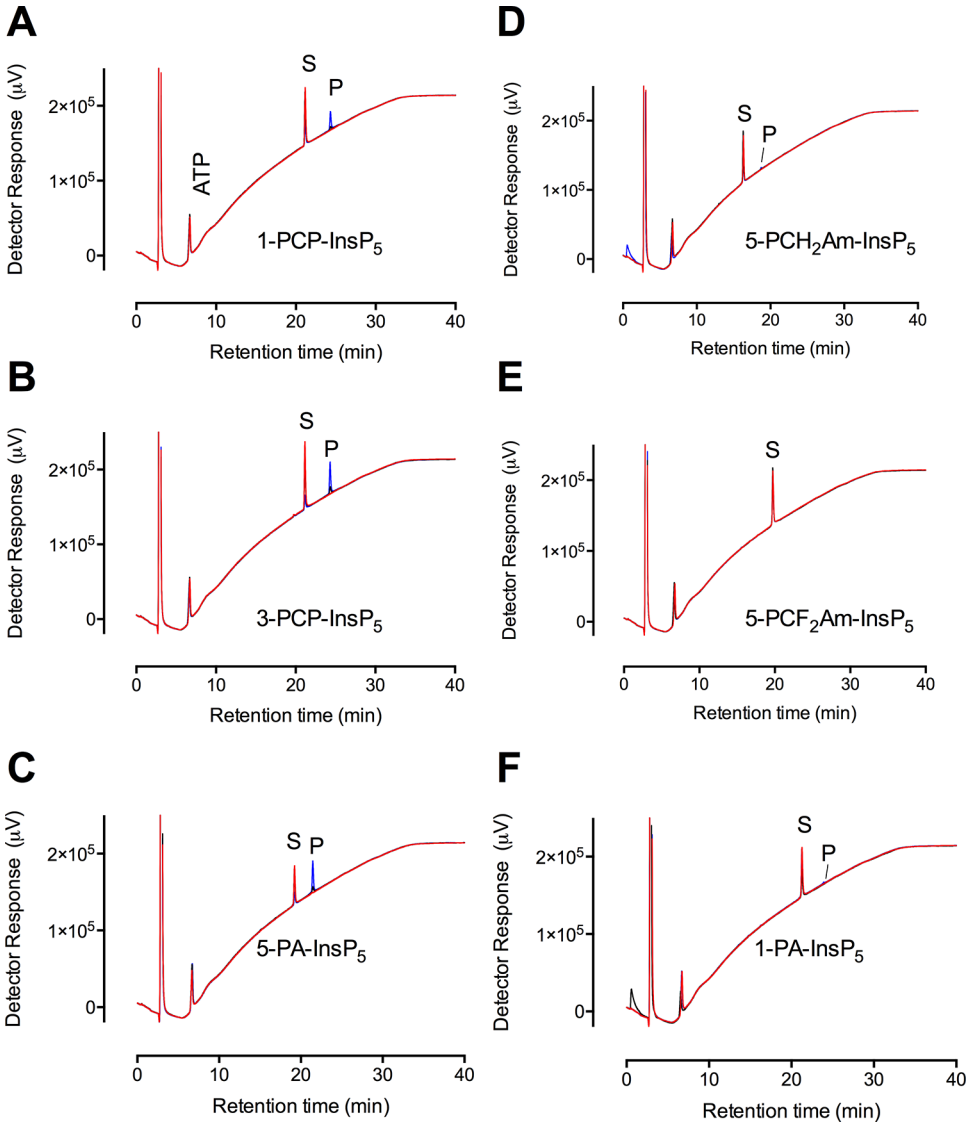

Figure 5. Phosphorylation of inositol pyrophosphate analogues by *St*ITPK1. HPLC resolution of products of reaction of *St*ITPK1 with ATP and (A) 1-PCP-Ins(2,3,4,5,6)P_5 [1-PCP-InsP_5]; (B) 3-PCP-Ins(1,2,4,5,6)P_5 [3-PCP-InsP_5]; (C) 5-PA-Ins(1,2,3,4,6)P_5 [5-PA-InsP_5]; (D) 5-PCH_2Am-Ins(1,2,3,4,6)P_5 [5-PCH_2Am-InsP_5]; (E) 5-PCF_2Am-Ins(1,2,3,4,6)P_5 [5-PCF_2Am-InsP_5]; (F) 1-PA-Ins(2,3,4,5,6)P_5 [1-PA-InsP_5]. Substrates are indicated, S; products, P. For all panels, chromatograms of reactions without enzyme are shown in red, 3 h incubations with enzyme are shown in black, and 12 h incubations in blue. The position of elution of ATP is shown in panel A. The HPLC column was eluted with a gradient of HCl.

of the inositol pyrophosphate- (5-PP-InsP_5) synthesizing activity of *St*ITPK1, even at a concentration, 5 μM, that is 2 orders of magnitude lower than the concentration of InsP_6 substrate. These data are consistent with the previous study of AtITPK1,[21] in which V_{max} with Ins(3,4,5,6)P_4 was 3 orders of magnitude greater than for InsP_6. These data provide a mechanism by which Ins(3,4,5,6)P_4 can regulate the phosphokinase activity of ITPK1. We speculate that Ins(3,4,5,6)P_4 competes with InsP_6 as substrate, both are found in plants[4,15,30] where Ins(3,4,5,6)P_4 is a precursor of InsP_6.[30,31] We further suggest that enhanced accumulation of Ins(3,4,5,6)P_4 in *itpk1* mutants[9,15,27] and *ipk1* mutants[4,15] amplifies reductions in PP-InsP species[9,15,27] that are widely reported to be the agents of much physiology.[3] Indeed, *itpk1* and *ipk1* mutants show a constitutive phosphate starvation response.[4,14,15]

DISCUSSION

Our understanding of inositol pyrophosphate function rests heavily on the molecular genetic disruption of hydroxy-kinase and phosphokinase activities. These have pleiotropic influence on plant physiology, reflecting involvement in processes as diverse as pathogen resistance, symbiosis, phosphate starvation response, and the action of plant growth regulators auxin and jasmonate. Disruption also has a multifaceted effect on inositol phosphate metabolism, with impacts on "lower" and "higher" inositol phosphates and inositol pyrophosphates alike. This is particularly apparent for ITPKs[9,15,27] and IP5K (IPK1).[4,15]

Ablation of *At*ITPK1 increases lower inositol phosphates[9,15,27] and reduces PP-InsP_5 and $[PP]_2$-InsP_4 alike, in plants. While it has been widely assumed that $[PP]_2$-InsP_4-synthesizing activity belongs exclusively to VIH1/2,[3,6,15,23,24,42] until the recent detailed description of noncanonical PP-InsP_5 species[9,21,27] little consideration had been given to other possibilities. Similarly, rather little consideration has been given

https://doi.org/10.1021/acs.biochem.3c00404
Biochemistry 2024, 63, 42−52

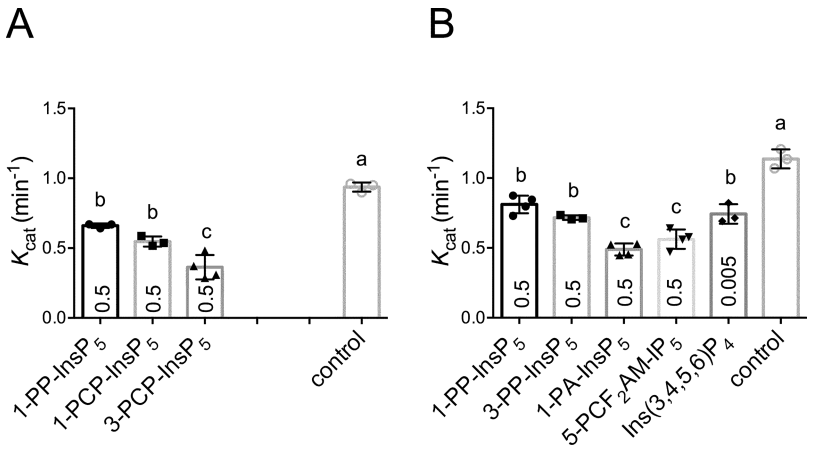

Figure 6. Inhibition of *St*ITPK1 phosphokinase activity by inositol pyrophosphate analogues. (A) Ins(1,2,3,4,5)P_5 5-phosphokinase activity; (B) InsP_6 5-phosphokinase activity. Reactions were performed for 2 h at 30 °C with 3 μM *St*ITPK1, 0.5 mM ATP, and 1 mM inositol phosphate in the absence or presence of competitor. The extent of inhibition at inhibitor concentration (mM) indicated by number in each column was estimated from the integrated peak areas of substrate and product peaks resolved by HPLC (example HPLC traces are shown in Figure S10). Significant difference at $p = 0.05$ between inhibitor treatments (by one-way ANOVA and Tukey's multiple comparisons test) is indicated by the absence of a common letter.

to the possibility that different inositol phosphates and inositol pyrophosphates are active site competitors of ATP-grasp kinases. With respect to the latter premise, the data presented here suggests that competition could be significant, and the principle likely applies to other ATP-grasp kinases. In respect of the former premise, the null hypothesis, that ITPK1 does not contribute directly (i.e., other than by provision of the 5-PP-InsP_5 substrate to VIH1/2) to [PP]$_2$-InsP_4 levels, is challenged. The pronounced inhibition of phosphokinase activity by Ins(3,4,5,6)P_4 says as much, while the reversibility of IPK1's phosphokinase activity (previously described for InsP_6 substrate,[21,27] here tested against 1-PP-InsP_5 and 3-PP-InsP_5) extends ITPK1 influence to whole cohorts of inositol pyrophosphate substrates that are widely reported in plants.[1−3,6−10,15,23,24,27,34,42] Taken together, the foregoing raises the possibility of adenine-nucleotide-(energy charge)-dependent substrate cycles between [PP]$_2$-InsP_4 and PP-InsP_5 species, offering extra dimension to the central role of ITPK1 in diverse physiological phenomena.[3−10] Nonetheless, recent work has also identified a family of plant and fungi-atypical dual specificity phosphatases (PFA-DSPs) that display activity against multiple inositol pyrophosphates. In vitro, they, like *At*ITPK1 and *St*ITPK1 here, show specificity for the removal of the β-5-phosphate of 5-PP-InsP_5, 1,5-[PP]$_2$-InsP_4, and 3,5-[PP]$_2$-InsP_4 alike.[34]

By corollary, it seems plausible that VIH1/2 also shows reversible phosphokinase (i.e., ATP-synthesizing) activity: not only does VIH1/2 possess the ATP-grasp fold but also the mammalian homologue PPIP5K2 shows ADP-driven 1,5-[PP]$_2$-InsP_4 1-dephosphorylation (ATP-synthesizing) activity.[28,43] It is, perhaps, instructive, therefore, to compare the relative activities of different ATP-grasp kinase proteins of plants. *At*VIH2 has been characterized as separate kinase and phosphatase domains.[24] The former shows 1-phosphokinase activity against InsP_6 and 5-PP-InsP_5 with turnover numbers of ~0.4 and ~1 (min^{-1}), respectively.[24] These constants were derived under assay conditions very similar to those employed in the present and earlier studies of *At*ITPK1.[21,27] K_{cat} for *At*ITPK1's phosphokinase activity against InsP_6, calculated from data,[20,21,27] is comparable, ~1.5 min^{-1}, here, for StITPK1, K_{cat} ~1.14 min^{-1} at pH 6.5. K_{cat} for 5-PP-InsP_5-driven ATP synthesis is greater.[27] Clearly, the energy charge acts through ITPK1 and other ATP-grasp kinases to modulate the levels of PP-InsP_5 and [PP]$_2$-InsP_4 that are widely reported to influence plant physiology. Indeed, genetic evidence shows that despite these very low K_{cat} values for both *At*ITPK1 and *At*VIH2, ablation of *At*ITPK1 markedly reduces the levels of PP-InsP_5 and [PP]$_2$-InsP_4 in plants,[9,27] while ablation of VIH1/2 markedly reduces [PP]$_2$-InsP_4.[8,24] The low cellular levels of these species, relative to InsP_6, typically less than 1%, perhaps implies that the bulk of cellular InsP_6 is accessible to *At*ITPK1. The difference in rate constants for 5-pyrophosphorylation and hydroxy-kinase activities may arise from poorer geometry for the former, with the placement of the receiving 5-phosphate or hydroxyl (for the latter) in different enzyme subsites.

CONCLUSIONS

The catalytic flexibility of the ATP-grasp fold kinase ITPK1 has been extended to include inositol pyrophosphates considered previously to be substrates/products of only VIH1/2, among kinases. Detailed analysis of the binding of diverse substrates and substrate analogues to *St*ITPK1 was enabled by the use of fluorescence polarization assays. This assay may find use for other ATP-grasp kinases. This and the solution of a nucleotide-liganded crystal structure for *St*ITPK1 offer an opportunity for more precise elaboration of inositol pyrophosphate function in plants, one that accommodates competition by substrates/inhibitors for cognate partners such as TIR1, COI1-ASK and COP signalosome components and enzymes alike. Plant ITPK1 also offers an opportunity for the study of ATP-grasp kinases in pyrophosphate biology contexts by provision of probes of phosphotransfer. One envisages the simple incorporation of ^{32}P or ^{33}P from γ-labeled ^{32}/^{33}P ATP into the β-5-phosphate of 1,5-[PP]$_2$-InsP_4 and 3,5-[PP]$_2$-InsP_4 and analogues thereof.

ASSOCIATED CONTENT

Supporting Information

The Supporting Information is available free of charge at https://pubs.acs.org/doi/10.1021/acs.biochem.3c00404.

https://doi.org/10.1021/acs.biochem.3c00404
Biochemistry 2024, 63, 42−52

Materials and methods; additional references; structures of inositol phosphates and analogues; HPLC traces; ligand binding and displacement curves; molecular models; data collection statistics; ligand interactions; and abbreviations (PDF)

Accession Codes

DNA and protein sequences can be obtained from TAIR (https://www.arabidopsis.org) and UniProt (https://www.uniprot.org/) under the accession numbers: *At*ITPK1 (At5g16760.1, NM_121682.3), *St*ITPK1 (EF362784, NM_001287863). Coordinates and diffraction data for *St*ITPK1 in complex with ADP and Mg^{2+} have been deposited in the PDB (https://www.rcsb.org/) with accession code 8OXE.

AUTHOR INFORMATION

Corresponding Authors

Charles A. Brearley − *School of Biological Sciences, University of East Anglia, Norwich NR4 7TJ, U.K.;* orcid.org/0000-0001-6179-9109; Email: c.brearley@uea.ac.uk

Andrew M. Hemmings − *School of Chemistry and School of Biological Sciences, University of East Anglia, Norwich NR4 7TJ, U.K.; College of Food Science and Technology, Shanghai Ocean University, Shanghai 201306, China;* Email: a.hemmings@uea.ac.uk

Authors

Hayley L. Whitfield − *School of Biological Sciences, University of East Anglia, Norwich NR4 7TJ, U.K.*

Raquel Faba Rodriguez − *School of Biological Sciences and School of Chemistry, University of East Anglia, Norwich NR4 7TJ, U.K.*

Megan L. Shipton − *Medicinal Chemistry & Drug Discovery, Department of Pharmacology, University of Oxford, Oxford OX1 3QT, U.K.;* orcid.org/0000-0002-9982-0927

Arthur W.H. Li − *School of Biological Sciences and School of Chemistry, University of East Anglia, Norwich NR4 7TJ, U.K.*

Andrew M. Riley − *Medicinal Chemistry & Drug Discovery, Department of Pharmacology, University of Oxford, Oxford OX1 3QT, U.K.;* orcid.org/0000-0001-9003-3540

Barry V.L. Potter − *Medicinal Chemistry & Drug Discovery, Department of Pharmacology, University of Oxford, Oxford OX1 3QT, U.K.;* orcid.org/0000-0003-3255-9135

Complete contact information is available at: https://pubs.acs.org/10.1021/acs.biochem.3c00404

Author Contributions

C.A.B.: conceptualization, funding acquisition, project administration, formal analysis, supervision, validation, investigation, visualization, methodology, TOC graphic, writing—original draft, writing—review and editing. A.M.H.: conceptualization, data curation, formal analysis, supervision, validation, investigation, visualization, methodology, writing—original draft, writing—review and editing. A.W.H.L.: investigation. B.V.L.P.: funding acquisition, supervision, investigation, methodology, writing—review and editing. A.M.R.: investigation, supervision, methodology, writing—review and editing. R.F.R.: data curation, formal analysis, validation, investigation. M.L.S.: investigation, methodology, writing—review and editing. H.L.W.: data curation, formal analysis, validation, investigation, visualization, methodology, writing—original draft, writing—review and editing.

Author Contributions

This work was funded in part by the Wellcome Trust. For the purpose of Open Access, the authors have applied a CC BY public copyright license to any author-accepted manuscript version arising from this submission.

Funding

This work was funded by the NERC through a grant ref. NE/W000350/1 to C.A.B. B.V.L.P. is a Wellcome Trust Senior Investigator (grant 101010).

Notes

The authors declare no competing financial interest.

ACKNOWLEDGMENTS

The authors would like to thank Emma Thompson, University of East Anglia, for the preparation of protein, Diamond Light Source for beamtime under proposal MX9475, and the staff of beamline i24 for assistance with crystal testing and data collection.

ABBREVIATIONS

*At*IPK1, IP5K, *Arabidopsis thaliana* inositol pentakisphosphate 2-kinase; *At*ITPK1, *Arabidopsis thaliana* inositol tris/tetrakisphosphate kinase 1; *At*ITPK4, *Arabidopsis thaliana* inositol tris/tetrakisphosphate kinase 4; D-*chiro*-$InsP_6$, 1-D-*chiro*-inositol 1,2,3,4,5,6-hexakisphosphate; EDTA, ethylenediamine tetraacetic acid; HEPES, 4-(2-hydroxyethyl)-1-piperazineethanesulfonic acid; His, histidine; HPLC, high-pressure liquid chromatography; *Eh*ITPK1, *Entamoeba histolytica* inositol tris/tetrakisphosphate kinase 1; *Hs*ITPK1, *Homo sapiens* inositol tris/tetrakisphosphate kinase 1; IP6K, inositol hexakisphosphate kinase; Ins(1,4,5,6)P_4, 1D-*myo*-inositol 1,4,5,6-tetrakisphosphate; Ins(3,4,5,6)P_4, 1D-*myo*-inositol 3,4,5,6-tetrakisphosphate; Ins(1,2,3,4,5)P_5, 1D-*myo*-inositol 1,2,3,4,5-pentakisphosphate; Ins(1,2,3,5,6)P_5, 1D-*myo*-inositol 1,2,3,5,6-pentakisphosphate; 1-$InsP_7$, 1-PP-$InsP_5$, 1D-1-diphospho-*myo*-inositol 2,3,4,5,6-pentakisphosphate; 2-FAM-$InsP_5$, 2-*O*-(2-(5-fluoresceinylcarboxy)-aminoethyl)-*myo*-inositol 1,3,4,5,6-pentakisphosphate (triethylammonium salt); 3-$InsP_7$, 3-PP-$InsP_5$, 1D-3-diphospho-*myo*-inositol 1,2,4,5,6-pentakisphosphate; 4-$InsP_7$, 4-PP-$InsP_5$, 1D-4-diphospho-*myo*-inositol 1,2,3,5,6-pentakisphosphate; 5-$InsP_7$, 5-PP-$InsP_5$, 5-diphospho-*myo*-inositol 1,2,3,4,6-pentakisphosphate; 6-$InsP_7$, 6-PP-$InsP_5$, 1D-6-diphospho-*myo*-inositol 1,2,3,4,5-pentakisphosphate; $InsP_8$, bis-diphospho-*myo*-inositol-tetrakisphosphate; 1,5-$InsP_8$, 1D-1,5-bis-diphospho-*myo*-inositol 2,3,4,6-tetrakisphosphate; 3,5-$InsP_8$, 1D-3,5-bis-diphospho-*myo*-inositol 1,2,4,6-tetrakisphosphate; MES, 2-(*N*-morpholino)ethanesulfonic acid; *neo*-$InsP_6$, *neo*-inositol 1,2,3,4,5,6-hexakisphosphate; NMR, nuclear magnetic resonance spectroscopy; OPLS, optimized potentials for liquid simulations; PAGE, polyacrylamide gel electrophoresis; PCR, polymerase chain reaction; PDB, Protein Data Bank; PEG 6000, polyethylene glycol 6000; PPIP5K, diphosphoinositol pentakisphosphate kinase; *rac*-$InsP_8$, 1:1 mixture of 1,5-$InsP_8$ and 3,5-$InsP_8$; *scyllo*-$InsP_6$, *scyllo*-inositol 1,2,3,4,5,6-hexakisphosphate; *St*ITPK1, *Solanum tuberosum* inositol tris/tetrakisphosphate kinase 1; TLS, translation-libration-screw-rotation; TLSMD, TLS, translation-libration-screw motion determination; VIH1, *Arabidopsis thaliana* diphosphoinositol pentakisphosphate kinase 1; VIH2, *Arabidopsis thaliana* diphosphoinositol pentakisphosphate kinase 2; VSGB, generalized Born

https://doi.org/10.1021/acs.biochem.3c00404
Biochemistry 2024, 63, 42−52

continuum solvent model; *Zm*ITPK1, *Zea mays* inositol tris/tetrakisphosphate kinase 1; 1-PCP-InsP_5, *myo*-inositol 2,3,4,5,6-pentakisphosphate-1-methylenediphosphonate; 3-PCP-InsP_5, *myo*-inositol 1,2,4,5,6-pentakisphosphate-3-methylenediphosphonate; 5-PA-InsP_5, *myo*-inositol 1,2,3,4,6-pentakisphosphate-5-phosphonoacetate; 5-PCH_2Am-InsP_5, 5-deoxy-5-(phosphonoacetamido)-*myo*-inositol 1,2,3,4,6-pentakisphosphate; 5-PCF_2Am-InsP_5, 5-deoxy-5-(phosphonodifluoroacetamido)-*myo*-inositol 1,2,3,4,6-pentakisphosphate; 5-PCP-InsP_5, *myo*-inositol 1,2,3,4,6-penta-phosphate-5-methylenediphosphonate; 1-PCP-5-PP-Ins(2,3,4,6)P_4, 5-diphospho-*myo*-inositol 2,3,4,6-tetrakisphosphate-1-methylenediphosphonate; 3-PCP-5-PP-Ins(1,2,4,6)P_4, 5-diphospho-*myo*-inositol 1,2,4,6-tetrakisphosphate-3-methylenediphosphonate

REFERENCES

(1) Parmar, P. N.; Brearley, C. A. Identification of 3- and 4-phosphorylated phosphoinositides and inositol phosphates in stomatal guard cells. *Plant Journal* **1993**, *4* (2), 255−263.

(2) Brearley, C. A.; Hanke, D. E. Inositol phosphates in barley (*Hordeum vulgare* L.) aleurone tissue are stereochemically similar to the products of breakdown of InsP_6 in vitro by wheat-bran phytase. *Biochem. J.* **1996**, *318* (Pt 1), 279−86.

(3) Riemer, E.; Pullagurla, N. J.; Yadav, R.; Rana, P.; Jessen, H. J.; Kamleitner, M.; Schaaf, G.; Laha, D. Regulation of plant biotic interactions and abiotic stress responses by inositol polyphosphates. *Front Plant Sci.* **2022**, *13*, No. 944515.

(4) Stevenson-Paulik, J.; Bastidas, R. J.; Chiou, S. T.; Frye, R. A.; York, J. D. Generation of phytate-free seeds in Arabidopsis through disruption of inositol polyphosphate kinases. *Proc. Natl. Acad. Sci. U. S. A.* **2005**, *102* (35), 12612−7.

(5) Wild, R.; Gerasimaite, R.; Jung, J. Y.; Truffault, V.; Pavlovic, I.; Schmidt, A.; Saiardi, A.; Jessen, H. J.; Poirier, Y.; Hothorn, M.; Mayer, A. Control of eukaryotic phosphate homeostasis by inositol polyphosphate sensor domains. *Science* **2016**, *352* (6288), 986−90.

(6) Dong, J.; Ma, G.; Sui, L.; Wei, M.; Satheesh, V.; Zhang, R.; Ge, S.; Li, J.; Zhang, T. E.; Wittwer, C.; Jessen, H. J.; Zhang, H.; An, G. Y.; Chao, D. Y.; Liu, D.; Lei, M. Inositol pyrophosphate InsP_8 acts as an intracellular phosphate signal in Arabidopsis. *Mol. Plant* **2019**, *12* (11), 1463−1473.

(7) Ried, M. K.; Wild, R.; Zhu, J.; Pipercevic, J.; Sturm, K.; Broger, L.; Harmel, R. K.; Abriata, L. A.; Hothorn, L. A.; Fiedler, D.; Hiller, S.; Hothorn, M. Inositol pyrophosphates promote the interaction of SPX domains with the coiled-coil motif of PHR transcription factors to regulate plant phosphate homeostasis. *Nat. Commun.* **2021**, *12* (1), 384.

(8) Laha, D.; Johnen, P.; Azevedo, C.; Dynowski, M.; Weiss, M.; Capolicchio, S.; Mao, H.; Iven, T.; Steenbergen, M.; Freyer, M.; Gaugler, P.; de Campos, M. K.; Zheng, N.; Feussner, I.; Jessen, H. J.; Van Wees, S. C.; Saiardi, A.; Schaaf, G. VIH2 regulates the synthesis of inositol pyrophosphate InsP_8 and Jasmonate-dependent defenses in Arabidopsis. *Plant Cell* **2015**, *27* (4), 1082−97.

(9) Laha, N. P.; Giehl, R. F. H.; Riemer, E.; Qiu, D.; Pullagurla, N. J.; Schneider, R.; Dhir, Y. W.; Yadav, R.; Mihiret, Y. E.; Gaugler, P.; Gaugler, V.; Mao, H.; Zheng, N.; von Wiren, N.; Saiardi, A.; Bhattacharjee, S.; Jessen, H. J.; Laha, D.; Schaaf, G. Inositol (1,3,4) trisphosphate 5/6 kinase1-dependent inositol polyphosphates regulate Auxin responses in Arabidopsis. *Plant Physiol* **2022**, *190* (4), 2722−2738.

(10) Gulabani, H.; Goswami, K.; Walia, Y.; Roy, A.; Noor, J. J.; Ingole, K. D.; Kasera, M.; Laha, D.; Giehl, R. F. H.; Schaaf, G.; Bhattacharjee, S. Arabidopsis inositol polyphosphate kinases IPK1 and ITPK1 modulate crosstalk between SA-dependent immunity and phosphate-starvation responses. *Plant Cell Rep* **2022**, *41* (2), 347−363.

(11) Sheard, L. B.; Tan, X.; Mao, H.; Withers, J.; Ben-Nissan, G.; Hinds, T. R.; Kobayashi, Y.; Hsu, F. F.; Sharon, M.; Browse, J.; He, S. Y.; Rizo, J.; Howe, G. A.; Zheng, N. Jasmonate perception by inositol-phosphate-potentiated COI1-JAZ co-receptor. *Nature* **2010**, *468* (7322), 400−5.

(12) Tan, X.; Calderon-Villalobos, L. I.; Sharon, M.; Zheng, C.; Robinson, C. V.; Estelle, M.; Zheng, N. Mechanism of auxin perception by the TIR1 ubiquitin ligase. *Nature* **2007**, *446* (7136), 640−5.

(13) Murphy, A. M.; Otto, B.; Brearley, C. A.; Carr, J. P.; Hanke, D. E. A role for inositol hexakisphosphate in the maintenance of basal resistance to plant pathogens. *Plant J.* **2008**, *56* (4), 638−52.

(14) Kuo, H. F.; Chang, T. Y.; Chiang, S. F.; Wang, W. D.; Charng, Y. Y.; Chiou, T. J. Arabidopsis inositol pentakisphosphate 2-kinase, *At*IPK1, is required for growth and modulates phosphate homeostasis at the transcriptional level. *Plant J.* **2014**, *80* (3), 503−15.

(15) Kuo, H. F.; Hsu, Y. Y.; Lin, W. C.; Chen, K. Y.; Munnik, T.; Brearley, C. A.; Chiou, T. J. Arabidopsis inositol phosphate kinases, IPK1 and ITPK1, constitute a metabolic pathway in maintaining phosphate homeostasis. *Plant J.* **2018**, *95* (4), 613−630.

(16) Fridy, P. C.; Otto, J. C.; Dollins, D. E.; York, J. D. Cloning and characterization of two human VIP1-like inositol hexakisphosphate and diphosphoinositol pentakisphosphate kinases. *J. Biol. Chem.* **2007**, *282* (42), 30754−62.

(17) Wilson, M. P.; Majerus, P. W. Isolation of inositol 1,3,4-trisphosphate 5/6-kinase, cDNA cloning and expression of the recombinant enzyme. *J. Biol. Chem.* **1996**, *271* (20), 11904−10.

(18) Josefsen, L.; Bohn, L.; Sorensen, M. B.; Rasmussen, S. K. Characterization of a multifunctional inositol phosphate kinase from rice and barley belonging to the ATP-grasp superfamily. *Gene* **2007**, *397* (1−2), 114−25.

(19) Caddick, S. E.; Harrison, C. J.; Stavridou, I.; Mitchell, J. L.; Hemmings, A. M.; Brearley, C. A. A *Solanum tuberosum* inositol phosphate kinase (*St*ITPK1) displaying inositol phosphate-inositol phosphate and inositol phosphate-ADP phosphotransferase activities. *FEBS Lett.* **2008**, *582* (12), 1731−7.

(20) Laha, D.; Parvin, N.; Hofer, A.; Giehl, R. F. H.; Fernandez-Rebollo, N.; von Wiren, N.; Saiardi, A.; Jessen, H. J.; Schaaf, G. Arabidopsis ITPK1 and ITPK2 have an evolutionarily conserved phytic acid kinase activity. *ACS Chem. Biol.* **2019**, *14* (10), 2127−2133.

(21) Whitfield, H.; White, G.; Sprigg, C.; Riley, A. M.; Potter, B. V. L.; Hemmings, A. M.; Brearley, C. A. An ATP-responsive metabolic cassette comprised of inositol tris/tetrakisphosphate kinase 1 (ITPK1) and inositol pentakisphosphate 2-kinase (IPK1) buffers diphosphoinositol phosphate levels. *Biochem. J.* **2020**, *477*, 2621−2638.

(22) Whitfield, H. L.; He, S.; Gu, Y.; Sprigg, C.; Kuo, H. F.; Chiou, T. J.; Riley, A. M.; Potter, B. V. L.; Hemmings, A. M.; Brearley, C. A. Diversification in the inositol tris/tetrakisphosphate kinase (ITPK) family: crystal structure and enzymology of the outlier *At*ITPK4. *Biochem. J.* **2023**, *480* (6), 433−453.

(23) Desai, M.; Rangarajan, P.; Donahue, J. L.; Williams, S. P.; Land, E. S.; Mandal, M. K.; Phillippy, B. Q.; Perera, I. Y.; Raboy, V.; Gillaspy, G. E. Two inositol hexakisphosphate kinases drive inositol pyrophosphate synthesis in plants. *Plant J.* **2014**, *80* (4), 642−53.

(24) Zhu, J.; Lau, K.; Puschmann, R.; Harmel, R. K.; Zhang, Y.; Pries, V.; Gaugler, P.; Broger, L.; Dutta, A. K.; Jessen, H. J.; Schaaf, G.; Fernie, A. R.; Hothorn, L. A.; Fiedler, D.; Hothorn, M. Two bifunctional inositol pyrophosphate kinases/phosphatases control plant phosphate homeostasis. *Elife* **2019**, *8*, No. e43582.

(25) Voglmaier, S. M.; Bembenek, M. E.; Kaplin, A. I.; Dorman, G.; Olszewski, J. D.; Prestwich, G. D.; Snyder, S. H. Purified inositol hexakisphosphate kinase is an ATP synthase: diphosphoinositol pentakisphosphate as a high-energy phosphate donor. *Proc. Natl. Acad. Sci. U. S. A.* **1996**, *93* (9), 4305−10.

(26) Phillippy, B. Q.; Ullah, A. H.; Ehrlich, K. C. Purification and some properties of inositol 1,3,4,5,6-Pentakisphosphate 2-kinase from immature soybean seeds. *J. Biol. Chem.* **1994**, *269* (45), 28393−9.

(27) Riemer, E.; Qiu, D.; Laha, D.; Harmel, R. K.; Gaugler, P.; Gaugler, V.; Frei, M.; Hajirezaei, M. R.; Laha, N. P.; Krusenbaum, L.;

https://doi.org/10.1021/acs.biochem.3c00404
Biochemistry 2024, 63, 42−52

Schneider, R.; Saiardi, A.; Fiedler, D.; Jessen, H. J.; Schaaf, G.; Giehl, R. F. H. ITPK1 is an $InsP_6$/ADP phosphotransferase that controls phosphate signaling in Arabidopsis. *Mol. Plant* **2021**, *14* (11), 1864−1880.
(28) Weaver, J. D.; Wang, H.; Shears, S. B. The kinetic properties of a human PPIP5K reveal that its kinase activities are protected against the consequences of a deteriorating cellular bioenergetic environment. *Biosci. Rep.* **2013**, *33* (2), No. e00022.
(29) Laha, D.; Portela-Torres, P.; Desfougeres, Y.; Saiardi, A. Inositol phosphate kinases in the eukaryote landscape. *Adv. Biol. Regul* **2021**, *79*, No. 100782.
(30) Brearley, C. A.; Hanke, D. E. Inositol phosphates in the duckweed *Spirodela polyrhiza* L. *Biochem. J.* **1996**, *314* (Pt 1), 215−25.
(31) Brearley, C. A.; Hanke, D. E. Metabolic evidence for the order of addition of individual phosphate esters in the *myo*-inositol moiety of inositol hexakisphosphate in the duckweed *Spirodela polyrhiza* L. *Biochem. J.* **1996**, *314* (Pt 1), 227−33.
(32) Bollmann, O.; Strother, S.; Hoffmann-Ostenhof, O. The enzymes involved in the synthesis of phytic acid in *Lemna gibba* (studies on the biosynthesis of cyclitols, XL. (1)). *Mol. Cell. Biochem.* **1980**, *30* (3), 171−5.
(33) Cosgrove, D. J. *Inositol phosphates - their chemistry, biochemistry and physiology*; Elsevier 1980.
(34) Gaugler, P.; Schneider, R.; Liu, G.; Qiu, D.; Weber, J.; Schmid, J.; Jork, N.; Haner, M.; Ritter, K.; Fernandez-Rebollo, N.; Giehl, R. F. H.; Trung, M. N.; Yadav, R.; Fiedler, D.; Gaugler, V.; Jessen, H. J.; Schaaf, G.; Laha, D. Arabidopsis PFA-DSP-Type phosphohydrolases target specific inositol pyrophosphate messengers. *Biochemistry* **2022**, *61* (12), 1213−1227.
(35) Watson, P. J.; Millard, C. J.; Riley, A. M.; Robertson, N. S.; Wright, L. C.; Godage, H. Y.; Cowley, S. M.; Jamieson, A. G.; Potter, B. V. L.; Schwabe, J. W. Insights into the activation mechanism of class I HDAC complexes by inositol phosphates. *Nat. Commun.* **2016**, *7*, 11262.
(36) Whitfield, H.; Hemmings, A. M.; Mills, S. J.; Baker, K.; White, G.; Rushworth, S.; Riley, A. M.; Potter, B. V. L.; Brearley, C. A. Allosteric site on SHIP2 identified through fluorescent ligand screening and crystallography: A potential new target for intervention. *J. Med. Chem.* **2021**, *64*, 3813−3826.
(37) Whitfield, H.; Gilmartin, M.; Baker, K.; Riley, A. M.; Godage, H. Y.; Potter, B. V. L.; Hemmings, A. M.; Brearley, C. A. A fluorescent probe identifies active site ligands of inositol pentakisphosphate 2-kinase. *J. Med. Chem.* **2018**, *61*, 8838−8846.
(38) Zong, G.; Shears, S. B.; Wang, H. Structural and catalytic analyses of the $InsP_6$ kinase activities of higher plant ITPKs. *FASEB J.* **2022**, *36* (7), No. e22380.
(39) Miller, G. J.; Wilson, M. P.; Majerus, P. W.; Hurley, J. H. Specificity determinants in inositol polyphosphate synthesis: crystal structure of inositol 1,3,4-trisphosphate 5/6-kinase. *Mol. Cell* **2005**, *18* (2), 201−12.
(40) Chamberlain, P. P.; Qian, X.; Stiles, A. R.; Cho, J.; Jones, D. H.; Lesley, S. A.; Grabau, E. A.; Shears, S. B.; Spraggon, G. Integration of inositol phosphate signaling pathways via human ITPK1. *J. Biol. Chem.* **2007**, *282* (38), 28117−25.
(41) Riley, A. M.; Deleu, S.; Qian, X.; Mitchell, J.; Chung, S. K.; Adelt, S.; Vogel, G.; Potter, B. V. L.; Shears, S. B. On the contribution of stereochemistry to human ITPK1 specificity: $Ins(1,4,5,6)P_4$ is not a physiologic substrate. *FEBS Lett.* **2006**, *580*, 324−330.
(42) Adepoju, O.; Williams, S. P.; Craige, B.; Cridland, C. A.; Sharpe, A. K.; Brown, A. M.; Land, E.; Perera, I. Y.; Mena, D.; Sobrado, P.; Gillaspy, G. E. Inositol trisphosphate kinase and diphosphoinositol pentakisphosphate kinase enzymes constitute the inositol pyrophosphate synthesis pathway in plants. *bioRxiv* **2019**, DOI: 10.1101/724914.
(43) Shears, S. B.; Baughman, B. M.; Gu, C.; Nair, V. S.; Wang, H. (2017) The significance of the 1-kinase/1-phosphatase activities of the PPIP5K family. *Adv. Biol. Regul.* **2017**, *63*, 98−106.

https://doi.org/10.1021/acs.biochem.3c00404
Biochemistry 2024, 63, 42−52